Sensors and Actuators A 148 (2008) 44–50

Contents lists available at ScienceDirect

Sensors and Actuators A: Physical

journal homepage: www.elsevier.com/locate/sna

Contactless electromagnetic excitation of resonant sensors made of conductive miniaturized structures

Marco Baù [a,*], Vittorio Ferrari [a], Daniele Marioli [a], Emilio Sardini [a], Mauro Serpelloni [a], Andrea Taroni [b]

[a] Department of Electronics for Automation, University of Brescia, Via Branze 38, 25123 Brescia (BS), Italy
[b] University "Carlo Cattaneo" - LIUC, C.so Matteotti, 22 - 21053 Castellanza (VA), Italy

ARTICLE INFO

Article history:
Received 5 February 2008
Received in revised form 14 June 2008
Accepted 27 June 2008
Available online 12 July 2008

Keywords:
Contactless sensors
Electromagnetic excitation
Eddy currents
Microresonators
Resonant sensors

ABSTRACT

An electromagnetic contactless excitation principle is presented to induce mechanical vibrations on miniaturized electrically conductive resonant structures to be used as passive sensors. An external coil arrangement generates a time-varying magnetic field which induces eddy currents on the structure surface. The interaction between the eddy currents and the magnetic field causes forces which can set the structure into vibration. The principle avoids any contact to the resonator structure to inject current and only requires the structure to be electrically conductive, without the need for specific magnetic properties. The principle is attractive for the development of passive sensors operating in environments with limited accessibility or incompatible with active electronics. A mathematical model of the excitation principle has been derived and has been supported by means of finite-element simulations. Experimental demonstration of the excitation principle has been obtained on cantilever and a clamped-clamped beam miniaturized conductive structures used as resonators. The readout of the vibrations has been performed by either piezoelectric and optical methods.

1. Introduction

Recently, increasing interest has been paid to sensors which can be contactless interrogated by an external unit. The lack of physical contact is attractive for applications in environments that are difficult to access and do not allow for cabled solutions, such as measurements inside the human body or in packages. Battery-powered systems are currently the most widespread solution, where active electronics and energy sources are located on both the sensing device and the interrogation unit. The main drawback of these systems is the necessity for periodical recharge/replacement of the sensor battery. As an alternative, the sensor and associated circuitry can be battery-less and powered by energy transfer from the reader [1], or by energy-harvesting from the environment [2].

As a further step, the availability of entirely passive sensing elements that can be externally excited and interrogated contactless without requiring active circuitry on board can be very attractive for a variety of applications. For example, contactless passive sensors can be desirable in hostile environments that can be incompatible with active electronics, such as high-temperature environments.

To this purpose, the exploitation of the resonance measurement principle to develop entirely passive structures used as basic sensing elements for a wide variety of measurands seems particularly promising. The working principle of a resonant sensor consists of measuring the frequency shift of an oscillating mechanical structure that can be brought into resonance using different actuating techniques, such as electrostatic, magnetic, electrothermal and piezoelectric [3]. The resonating principle is effective because measurement information is carried by the frequency of the readout signal and not by its magnitude. In particular, the resonance frequency does not depend on the specific interrogation method adopted, making resonant sensing a robust approach for contactless operation.

In the following, the magnetic actuation principle will be considered as a mean to contactless excite mechanical resonances in miniaturized passive structures. Magnetic actuation can be usually obtained by either using an external static magnetic field and exploiting the Lorentz forces arising from time-variant currents driven into conductor paths present in the structure [4–7], or by using an external time-variant magnetic field that interacts with magnetic films that need to be deposited on the resonant structure [8–10]. In the perspective of realization of the sensors in MEMS technology, the use of magnetic films added on the sensing structure has the drawback of requiring special materials and dedicated processing steps. In particular, magnetic films may have compatibility limitations with the standard CMOS fabrication process, both

* Corresponding author. Tel.: +39 030 3715896; fax: +39 030 380014.
E-mail address: marco.bau@ing.unibs.it (M. Baù).

0924-4247/$ – see front matter © 2008 Elsevier B.V. All rights reserved.
doi:10.1016/j.sna.2008.06.034

causing contamination in the existing structure and presenting adhesion problems [11].

As an alternative, in the present work we investigate the possibility to exploit a time-variant external magnetic field to induce vibrations and mechanical resonance on structures that are only required to be electrically conductive, while they do not require specific magnetic properties. In this way, the resonant element is passive and electrically conductive, while the excitation is supplied externally [12].

The method of electromagnetic excitation has been verified on three different electrically conductive structures represented by an aluminum sheet placed on a piezoelectric bimorph cantilever, a titanium cantilever, and a titanium clamped-clamped beam. At first, the piezoelectric effect of the bimorph cantilever has been exploited as a mean to detect the vibrations induced in the attached aluminum sheet. Subsequently, in the two latter cases, the induced vibrations have been detected by a contactless optical system previously developed for the characterization of resonators vibrating in out-of-plane mode [13]. In the experimental tests, the magnetic field has been generated by a solenoid with a ferrite core having a cylinder bar geometry. A mathematical model for the excitation principle has been proposed and verified by both finite-element simulations and experimental tests.

2. Operating principle

In Fig. 1 a schematic diagram of the contactless electromagnetic method for the mechanical excitation of a conductive structure is presented. A conductive plane resonator, represented in the drawing by a cantilever, is placed in the region where a magnetic field $B(t)$ generated by an external coil is present. The origin of the xyz axes is placed at the intersection of the longitudinal axis of the coil with the plane of the cantilever, which is assumed to be clamped at its end on the negative side of the y-axis. The solenoid geometry of the coil has been selected to produce a magnetic field that on the surface of the conductor has both vertical and radial components, directed along the z-axis and in the xy plane, respectively. As a first simplifying assumption, the conductive layer can be assumed to be an infinitely thin surface. If the current $I_e(t)$ driven in the coil is varying sinusoidally with angular frequency ω, assuming a linear behavior of the core, the magnetic field vector $B(t)$ on the conductive surface can be expressed in general as

$$B(t) = B_e \cos(\omega t) \tag{1}$$

where B_e is the amplitude of the sinusoidal field due to $I_e(t)$. The flux $\Phi(B)$ of the magnetic field B through the conductive layer only depends on the vertical component B_z of the magnetic field. Without loss of generality, for the scope of the present analysis, it can be assumed that B_z is uniform over an area A of the conductive layer facing the solenoid.

Therefore, for the Faraday's law, the following electromotive force $V_i(t)$ proportional to the time derivative of $\Phi(B_z)$ is generated along closed circular paths on the conductive surface, as reported in Fig. 1:

$$V_i(t) = -\frac{\mathrm{d}\Phi(B_z)}{\mathrm{d}t} = -A\frac{\mathrm{d}B_z(t)}{\mathrm{d}t} = AB_{ez}\omega\ \sin(\omega t) \tag{2}$$

The electromotive force $V_i(t)$ generates eddy currents in the conductive layer. If now a finite thickness of the conductive layer is considered, the distribution of the eddy-current density along the thickness, for a given layer material, depends on the excitation frequency [14]. It can be anticipated that, as it will be quantitatively shown in the following sections, at the frequency of interest in the present study (in the order of 1 kHz) the electromagnetic penetration depth in common conducting materials is much larger than the adopted layer thickness (in the order of 100 μm). As a consequence, the eddy-current density does not significantly depend on the z coordinate, therefore it can be assumed to be uniform throughout the thickness of the conductive layer. The magnitude and phase of the eddy-current density $J(t)$ depend on the complex electrical impedance $Z(\omega) = |Z(\omega)| \exp(\mathrm{j}\phi(\omega))$ of the conductive layer at the excitation angular frequency ω. Therefore

$$J(t) = \frac{AB_{ez}\omega}{S|Z(\omega)|}\sin(\omega t + \phi) = k(\omega)\sin(\omega t + \phi) \tag{3}$$

where S is the equivalent cross-section area of the current path in the conductive layer. The eddy currents $J(t)$ interact with the overall magnetic field $B(t)$ generating Lorentz forces per unit volume $F(t)$ given by the vector product $F(t) = J(t) \times B(t)$, which act on the cantilever. In this case, the component J_z of the eddy-current density vector along z is zero, therefore the components of the Lorentz force are

$$\begin{aligned} F_x &= J_y B_z - J_z B_y = J_y B_z, \\ F_y &= -J_x B_z + J_z B_x = -J_x B_z, \\ F_z &= J_x B_y - J_y B_x \end{aligned} \tag{4}$$

where the implicit sinusoidal time dependence of all quantities has been omitted for easier notation.

From Eq. (4) the components F_x and F_y combine to create a force radially oriented in the xy plane, while the component F_z acts along the z direction. Taking into account the sinusoidal time dependence, the resulting expression of $F_z(t)$ is the following:

$$F_z(t) = \tfrac{1}{2}k(\omega)B_{er}[\sin(\phi) + \sin(2\omega t + \phi)] \tag{5}$$

where $B_{er} = \sqrt{B_{ex}^2 + B_{ey}^2}$ is the magnitude of the sinusoidal components of the magnetic field along the radial axis. It can be observed that the force is proportional to B_{er} and it is composed of a sinusoidal term at angular frequency 2ω, plus a DC term dependent on the phase of the electrical impedance of the conductive layer.

The time-dependent component of the force $F_z(t)$ can excite the cantilever into flexural vibrations. Apart from the geometry, the

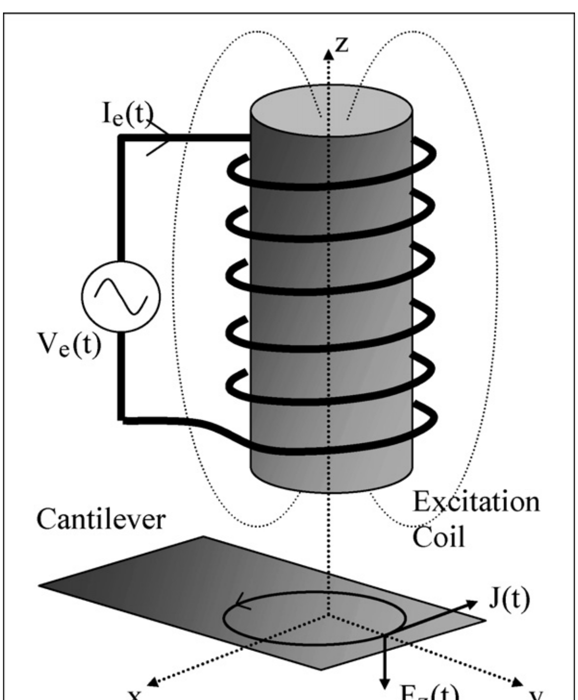

Fig. 1. Schematic diagram of the operating principle.

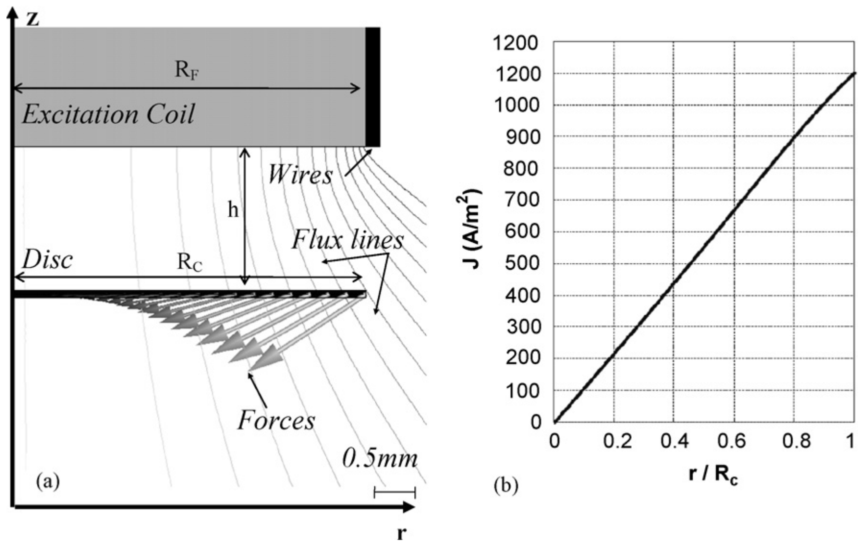

Fig. 2. Simulation of eddy currents and forces on the conductive disc at time of one period T of the excitation current: (a) forces and flux lines and (b) eddy currents versus the r coordinate normalized to the conductive surface radius.

principle is the same as in electromagnetic acoustic transducers (EMATs) [15–17] or in direct magnetic generation of acoustic waves in microsensors [18]. In all such applications, however, a static magnetic field is generally applied, which is typically done by means of permanent magnets. On the contrary, the present work investigates the case where magnets are absent and no external static magnetic field is applied, i.e. $B(t)$ is a sinusoidal zero-mean field. In this case, according to Eq (5), to excite a vibration mode of a resonator at angular frequency ω_r the excitation coil must be driven at an angular frequency ω so that $\omega_r = 2\omega$.

Regarding the static component of the force F_z, since the conductive layer is sufficiently thin that the effects related to the skin depth can be neglected, its electrical impedance $Z(\omega)$ is predominantly resistive [19], therefore in the expression (5) ϕ is nearly zero and no significant DC term in F_z is expected.

3. Simulation results

Finite-element simulations on the system geometry described in Fig. 1 have been executed to study the behavior of the forces that arise on a conductive structure from the interaction between the contactless-induced eddy currents and the magnetic field. The software used is Maxwell 2D by Ansoft, which readily allows to simulate systems with cylindrical symmetry and with time-variant electromagnetic sources. Therefore, the geometry used for the experimental setup has been simplified into a cylindrical symmetry, modeling the resonator as a conductive disc located under a linear solenoid. The adopted simplified model, where the conductive beam is replaced by a conductive disc, is functionally equivalent to the real one, provided that the disk diameter is equal to the width of the cantilever. The resonator is a titanium disc (relative permeability $\mu_r = 1.00018$ and electrical conductivity $\sigma = 2.1 \times 10^6$ S/m) with thickness of 100 μm positioned under the ferrite core in central axial position. The excitation solenoid is modeled as one single equivalent copper winding of 0.1 mm wounded around a cylindrical ferrite core ($\mu_r = 1000$) with diameter and length of 9 and 50 mm, respectively. The excitation source is an AC cosine current flowing into the winding with peak amplitude and frequency of 1 A and 800 Hz, respectively.

In Fig. 2(a) the vertical axis z represents the symmetry axis of the cylindrical solenoid and coincides with the z-axis of Fig. 1, while the r-axis identifies the radial direction. The drawing in Fig. 2(a) shows (i) the solenoid, (ii) the conductive disc, and (iii) the simulated quantities, namely force vectors F and flux lines of the magnetic field B. The arrows in the image represent the instantaneous magnitudes of force at one fixed time of the excitation current cycle. The diagram in Fig. 2(b) represents the magnitude of eddy-current density vector J in the conductive layer, which is oriented along the angular coordinate θ, versus the radial coordinate r normalized to the layer radius R_C. It can be observed that the magnitude of the eddy-current density increases with increasing the ratio r/R_C with an almost linear dependence.

Fig. 3 shows the diagrams of the vertical and radial components f_z and f_r of the Lorentz force at different values of distance h between the resonator plane and the ferrite core normalized to the radius R_F. The forces f_z and f_r are the results of the integration of the forces per unit volume F_z and $F_r = \sqrt{F_x^2 + F_y^2}$ of Eq. (4) over a vertical cross-section whose length is the radius of the conductive layer. The forces are plotted normalized to the maximum value of the radial force. For the adopted dimensions, the radii R_F and R_C of the ferrite core and the conductive disc, respectively, are equal. The resulting vertical component f_z of the force presents a maximum for a normalized distance of 0.08. This behavior is qualitatively justified considering that the amplitude of the current density J decreases monotonically when the distance increases, while the amplitude of the radial magnetic field B_{er} increases from a null value up to a maximum and then decreases.

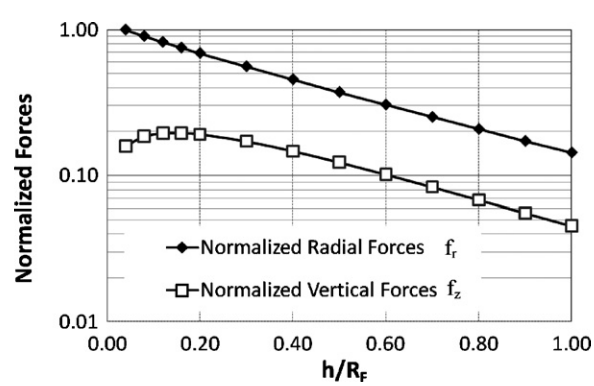

Fig. 3. Simulation results of the normalized vertical and radial forces f_z and f_r versus the normalized distance.

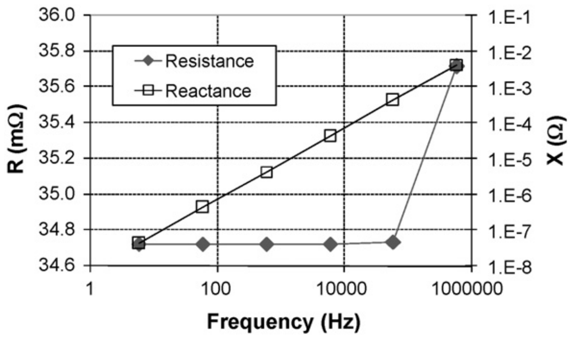

Fig. 4. Simulation results of the cantilever resistance and reactance at different frequencies.

Table 1
Phase values of $Z(f)$ calculated using the simulation results of Fig. 4

Frequency	Impedance phase (°)
6 Hz	0.0004
60 Hz	0.0045
600 Hz	0.0448
6 kHz	0.4478
60 kHz	4.4676
600 kHz	36.9501

The impedance $Z(f)$ associated to the eddy-current closed paths on the conductive layer as a function of the frequency has also been evaluated by simulations. The impedance is assumed to be modeled by a resistance R in series with a reactance X, both of which may depend on frequency. The simulator employs an energetic method to evaluate both R and X [20].

Fig. 4 shows the simulation results for the resistance $R(f)$ and the reactance $X(f)$ computed at different frequencies ranging from 6 Hz to 600 kHz, while in Table 1 the resulting phase ϕ of $Z(f)$ is derived. It can be observed that, at least up to 6 kHz the phase shift ϕ is well below 1° which implies that the behavior of the conductive disc is essentially resistive. This result, in turn, justifies the assumption made in Section 2 about the independence of the eddy-current density J on the z coordinate [19].

4. Experimental setup

Two different experimental setups have been employed to verify the described principle. Fig. 5 shows a detailed diagram of the first experimental setup used, where an aluminum thin sheet has been applied on a piezoelectric bimorph cantilever with dimensions of 15 mm × 1.5 mm × 0.6 mm. A waveform generator (Agilent 33220A) with low harmonic distortion feeds a purposely developed power amplifier to drive the exciting coil up to a maximum peak-to-peak

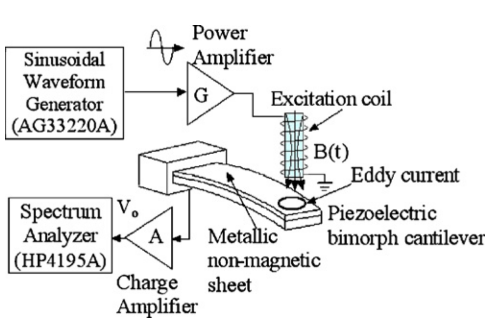

Fig. 5. Diagram of the experimental setup employed with the piezoelectric bimorph cantilever.

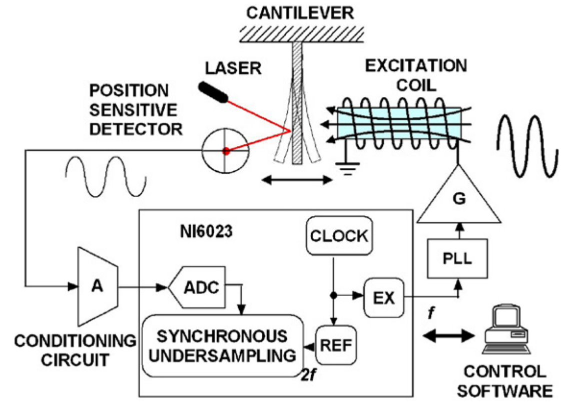

Fig. 6. Diagram of the experimental setup employing the optical characterization system.

amplitude of 110 V. The solenoid coil is composed of about 1000 turns of copper wire of 0.1 mm diameter wounded around a cylindrical ferrite core (Fair-Rite no. 3078990911) with diameter and length of 9 and 50 mm, respectively. A frequency characterization of the coil has been performed by means of an impedance analyzer (HP4194A), resulting in a series resistance R_s of 150 Ω and a series inductance L_s of 223 mH measured at the frequency of 1 kHz. The signal from the piezoelectric bimorph cantilever has been conditioned by a charge amplifier with a gain of $0.3 \times 10^{12}\,F^{-1}$, and the output signal V_o has been fed to a spectrum analyzer (HP4195A) for readout.

For the tests carried out on metallic beam resonators, a different setup has been used which does not include the piezoelectric bimorph as the vibration detector. The setup is based on an optical system previously described in [13] whose block diagram is shown in Fig. 6. In the current setup, the system generates a swept-frequency excitation signal EX which is converted to a sinusoidal signal V_C by a Phase-Locked Loop (PLL) and fed to a power amplifier of gain G to drive the coil at frequency f. The mechanical vibrations of the resonator are detected by means of an optical triangulator composed of a laser diode and a position sensitive detector. The readout signal from the triangulator undergoes synchronous undersampling to derive the real and imaginary components of the frequency response of the resonator. By properly setting the internal synchronization mechanism REF, a synchronous demodulation is performed locking on the component at frequency $2f$ of the readout signal. The processing is equivalent to a synchronous demodulation with lock-in detection. To allow simultaneous magnetic excitation and optical detection, one side of the metallic resonator has been faced to the excitation coil, while the opposite one has been used as a reflecting surface for the laser.

5. Experimental results

With the experimental apparatus described in Fig. 5, the conductive layer placed on the piezoelectric bimorph cantilever has been excited at five different frequencies, namely 700, 720, 735, 750, and 770 Hz. In this frequency range the current circulating in the coil is 37 mA rms with a peak-to-peak applied voltage of 110 V. The results obtained from the five different excitation frequencies are, in the following, labeled with sequential numbers from 1 to 5, respectively. Fig. 7 shows the superimposed view of the measured spectra of the readout signal V_o in the five excitation conditions. For each of the labeled excitation conditions, two peaks, one in the lower frequency band and the other in the higher, are detected in the spectra of the readout signal.

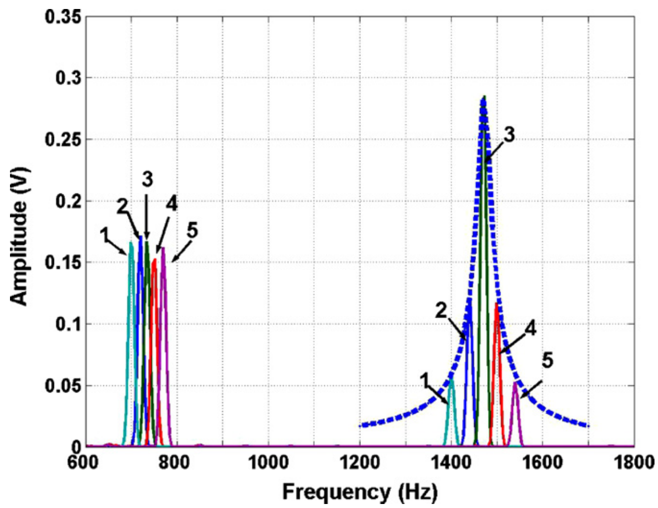

Fig. 7. Superimposed view of the spectra of the readout signal V_o in the case of no drops on the piezoelectric bimorph cantilever tip.

In the high part of the frequency range the peaks are detected at twice the excitation frequency as expected, i.e. at 2*f*. The envelope of the peaks at 2*f* shows a resonance trend with resonance frequency f_r at 1470 Hz, corresponding to an excitation frequency *f* of 735 Hz. The measured resonance frequency f_r is in good agreement with the value derived from the independent measurement of the real part of the electrical admittance $G = \mathrm{Re}(Y)$ of the piezoelectric bimorph cantilever, carried out with a HP4194A impedance analyzer, taken as reference and shown in diagram A of Fig. 8. In Fig. 7, peaks are also visible in the low part of the frequency range corresponding to the different values of the excitation frequency *f*. According to the theory illustrated in Section 2, peaks at the excitation frequency *f* are unexpected. The presence of such peaks, considering the evidence that they are all similar in amplitude irrespective of the excitation frequency, can be reasonably attributed to the coupling through parasitic elements between the excitation coil and the readout circuit.

To further verify that the piezoelectric bimorph cantilever is indeed mechanically excited, drops of paint have been used as loading masses on the tip of the cantilever in order to decrease its resonance frequency. The drop masses are estimated in the order of a milligram, i.e. much lower than the cantilever rest mass, yet their accurate value is irrelevant here, since they are merely intended as a convenient mean to induce a detectable downshift of the resonance frequency without appreciably perturbing the vibration mode shape. Diagram B in Fig. 8 shows how the resonance frequency, measured by the impedance analyzer, has decreased by adding a mass equivalent to two drops of paint.

After mass loading, the spectra of the readout signal V_o have been measured again for excitation frequencies of respectively 660, 670, 680, 690, and 700 Hz. In this case the current in the coil is 40 mA rms with peak-to-peak voltage of 110 V.

Fig. 9 shows the envelopes of the peaks at 2*f* for the unloaded and loaded cases. For the case with mass loading the envelope is centered at 1361 Hz, which is in good agreement with the resonance value identified by the conductance measurement reported in plot B of Fig. 8.

Subsequently, the experimental tests have been conducted using the experimental apparatus of Fig. 6 with a titanium cantilever as the resonator. The cantilever has dimensions of 100 μm × 10 mm × 1.4 mm. Titanium has Young's modulus *E* of 105×10^9 Pa, mass density ρ of 4940 kg/m^3 and electrical conductivity σ of 2.1×10^6 S/m. Preliminarily, the cantilever resonance frequency has been evaluated by analyzing the time response of the cantilever to an applied mechanical impulse. A resonant frequency of about 700 Hz has been thereby estimated which is in good agreement with the analytical model which, for the first flexural mode, predicts:

$$f_0 = 0.55966\sqrt{\frac{EI}{\rho L^3}} = 745\,\mathrm{Hz}$$

where *L* and *I* are, respectively, the length of the cantilever and the moment of inertia of the section [21].

Afterwards, the resonator has been excited by means of the same coil used in the previous setup, while the movement has been measured by the optical system. The displacement of the beam has been measured by driving the excitation coil with a sinusoidal current of 87 mA rms in the range 225–425 Hz, while the readout signal from the triangulator has been read at 2*f*, i.e. in the range 450–850 Hz.

As in the previous experiment, minute drops of paint have been used as loading masses on the tip of the cantilever to decrease the resonance frequency. Fig. 10 shows the frequency response of the cantilever tip displacement normalized to its peak value in the cases

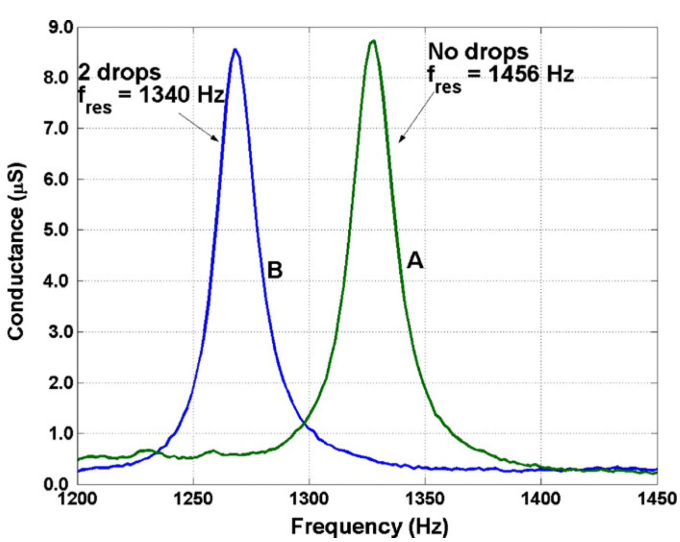

Fig. 8. Electrical conductance diagram of the piezoelectric bimorph cantilever in the case of no drops (A) and with two drops (B) on the tip.

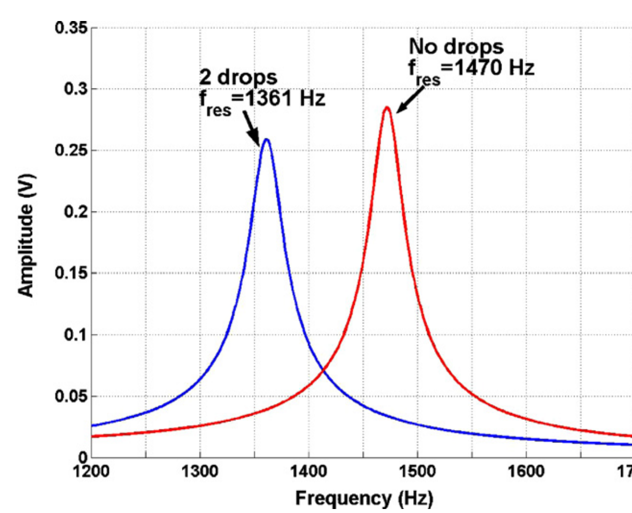

Fig. 9. Superimposed view of the envelopes at frequency 2*f* of the readout signal V_o in the case of no drops and two drops on the piezoelectric bimorph cantilever tip.

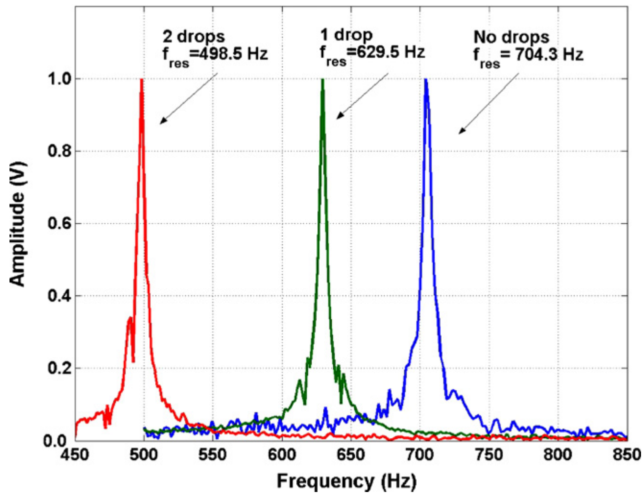

Fig. 10. Variations of the resonance frequency of the titanium cantilever.

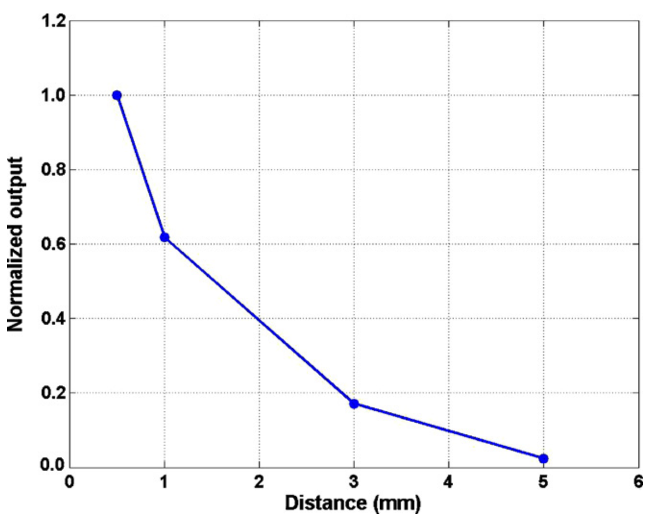

Fig. 11. Normalized peak amplitudes of the frequency response at resonance versus the distance of the excitation coil.

of no drops, one drop and two drops, respectively. As expected the resonance frequency f_{res} progressively decreases with increasing the amount of the added mass.

By means of a micrometric stage the distance between the coil and the cantilever has been varied and for each distance the frequency response of the resonator displacement has been measured. Fig. 11 shows the frequency response amplitudes measured at resonance, normalized to the maximum value, as a function of the distance. A non-linear decreasing trend can be observed with a decrement of about 97% over a distance variation of 4.5 mm.

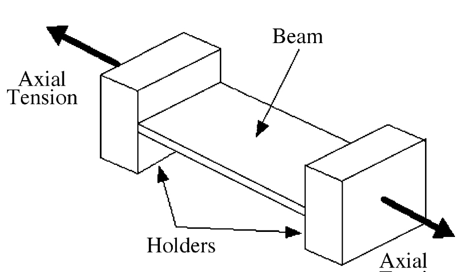

Fig. 12. Schematic drawing of the clamped-clamped beam.

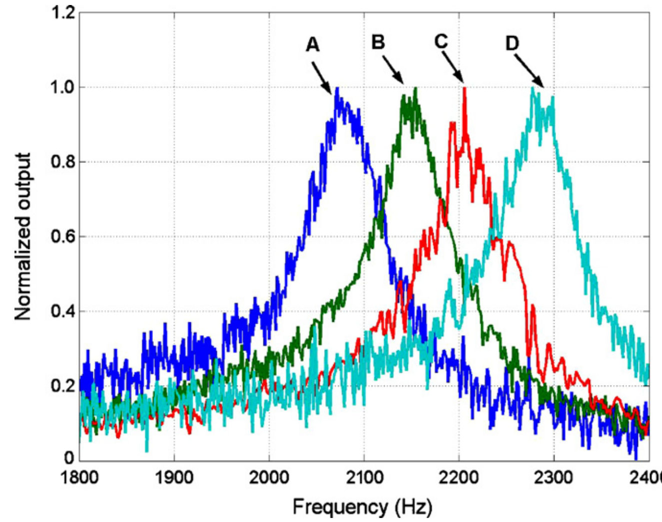

Fig. 13. Variations of the frequency response of the clamped-clamped beam.

Fig. 12 shows a schematic drawing of a further resonator geometry employed to verify the principle. In this case, a tunable resonator has been built using a 100-μm thick clamped-clamped titanium beam with lateral dimensions of 17 mm × 1.4 mm mounted between two clamping holders. By applying an axial tension to the beam, the resonance frequency can be changed.

A measurement with no axial tension has been performed by exciting the coil in the range 950–1200 Hz with a current of 26 mA rms, detecting a resonance frequency of 2070 Hz as shown in curve A of Fig. 13. In the same figure the curves labeled B–D show the frequency response of the resonator displacement with three increasing axial tensions applied. As expected, when the axial tension of the beam is increased a corresponding frequency up-shift is observed.

6. Conclusions

In this work the possibility to induce vibrations in a contactless way on conductive and non-magnetic structures by an external time-changing magnetic field has been analyzed and experimentally demonstrated. The force acting on the structures arises from the interaction between the eddy currents, induced in the conductive layer by the time-changing magnetic field, and the magnetic field itself. This approach, besides avoiding any contact to the resonators to inject current, does not require a static magnetic field, therefore the need for poling magnets is avoided. The theoretical predictions have been first confirmed by simulations, and then experimentally verified on prototypes of miniaturized structures. The proposed principle can be in general applied to measure a large variety of physical quantities which can cause a predictable shift in the resonant frequency of a suitable miniaturized structure. Examples can be for instance tensile strain, which in turn can be used to measure force and pressure, or added amount of mass, which could yield to microbalance sensors. The activity is now investigating the effect of the geometrical parameters of the resonant structures on the excitation mechanism, and the possibility to also readout the vibrations via the electromagnetic effect. A first attempt has been proposed in [22] based on an additional dual-coil arrangement, which applies and senses a probing magnetic field at higher frequency and exploits it to measure the magnetic field generated by oscillation. Perspective applications of the work is to transfer the principle to microfabricated structures working as passive and robust sensing elements that can be contactless interrogated over a short range.

References

[1] E. Abad, et al., Flexible tag microlab development: gas sensors integration in RFID flexible tags for food logistic, Sens. Actuators B 127 (2007) 2–7.
[2] J.A. Paradiso, T. Stamer, Energy scavenging for mobile and wireless electronics, in: Pervasive Computing, January–March, 2005, pp. 18–27.
[3] O. Brand, CMOS-based resonant sensors, in: Proceedings of IEEE Sensors 2005, Irvine, CA, October 31–November 3, 2005.
[4] S. Baglio, L. Latorre, P. Nouet, Resonant magnetic field microsensors in standard CMOS technology, in: IMTC/1999, 1999, pp. 452–457.
[5] A.B. Temnykh, R.V.E. Lovelace, Electro-mechanical resonant magnetic field sensors, Nucl. Instrum. Meth. 484 (2002) 95–101.
[6] A. Nannini, D. Pacia, F. Pieri, P. Toscano, A CMOS—compatible bulk technology for the fabrication of magnetically actuated microbalances for chemical sensing, Sens. Actuators B 118 (2006) 343–348.
[7] D.W. Lee, Y.L. Lee, J.H. Kang, Fabrication and evaluation of a novel protein sensor based on Lorentz force, Microelectron. Eng. 84 (2007) 1719–1723.
[8] J.W. Judy, R.S. Muller, Magnetic microactuation of torsional polysilicon structures, Sens. Actuators A 53 (1996) 392–397.
[9] T. Ono, M. Esashi, Magnetic force and optical force sensing with ultrathin silicon resonator, Rev. Sci. Instrum. 74 (2003) 5141–5146.
[10] D. Then, A. Vidic, Ch. Ziegler, A highly sensitive self-oscillating cantilever array for the quantitative and qualitative analysis of organic vapor mixtures, Sens. Actuators B 117 (2006) 1–9.
[11] M.R.J. Gibbs, Applications of magmems, J. Magn. Magn. Mater. 290–291 (2005) 1298–1303.
[12] C. De Angelis, V. Ferrari, D. Marioli, E. Sardini, M. Serpelloni, A. Taroni, Magnetically induced oscillations on a conductive cantilever for resonant microsensors, Sens. Actuators A 135 (2007) 197–202.
[13] M. Baù, V. Ferrari, D. Marioli, A. Taroni, Cost-effective system for the characterization of microstructures vibrating in out-of-plane modes, Sens. Actuators A 142 (2008) 270–275.
[14] H.A. Wheeler, Formulas for the skin effect, in: Proceedings of I.R.E., 1942, pp. 412–424.
[15] S. Dixon, S.B. Palmer, Wideband low frequency generation and detection of Lamb and Rayleigh waves using electromagnetic acoustic transducers (EMATs), Ultrasonics 42 (2004) 1129–1136.
[16] K. Kawashima, Theory and numerical calculation of the acoustic field produced in metal by electromagnetic ultrasonic transducer, J. Acoust. Soc. Am. 60 (5) (1976) 1089–1099.
[17] K. Kawashima, O.B. Wright, Resonant electromagnetic excitation and detection of ultrasonic waves in thin sheets, J. Appl. Phys. 72 (10) (1992) 4830–4839.
[18] F. Lucklum, P. Hauptmann, N.F. De Rooij, Magnetic direct generation of acoustic resonances in silicon membranes, Meas. Sci. Technol. 19 (2006) 719–726.
[19] Y. Le Bihan, Study on the transformer equivalent circuit of eddy current nondestructive evaluation, NDT&E International 36 (2003) 297–302.
[20] Ansoft Maxwell 2D Field Simulator v12 User's Guide, Eddy current Application Note (Chapter 6.1).
[21] V. Ferrari, D. Marioli, A. Taroni, E. Ranucci, P. Ferruti, Development and application of mass sensors based on flexural resonances in alumina beams, IEEE Trans. Ultrason. Ferroelectr. Freq. Control 43 (4) (1996) 601–608.
[22] M. Baù, V. Ferrari, D. Marioli, E. Sardini, M. Serpelloni, A. Taroni, Contactless excitation and readout of passive sensing elements made by miniaturized mechanical resonators, in: Proceedings of IEEE Sensors 2007, Atlanta, October 28–31, 2007, pp. 36–39.

Biographies

Marco Baù was born in Castiglione delle Stiviere, Italy, in 1981. In 2005 he received the Laurea degree in Electronic Engineering cum laude at the University of Brescia. Since November 2005 he has been a PhD student in "Electronic Instrumentation" at the University of Brescia. His main research activity deals with the design of electronics circuit and the development of techniques for the contactless activation and detection of resonant sensors with particular regard to MEMS resonators.

Vittorio Ferrari was born in Milan, Italy, in 1962. In 1988 he obtained the Laurea degree in Physics cum laude at the University of Milan. In 1993 he received the Research Doctorate degree in Electronic Instrumentation at the University of Brescia. Since 2006, he has been a full professor of Electronics at the Faculty of Engineering of the University of Brescia. His research activity is in the field of sensors and the related signal-conditioning electronics. Topics of interest are acoustic-wave piezoelectric sensors, microresonant sensors and MEMS, autonomous sensors and power scavenging, oscillators for resonant sensors and frequency–output interface circuits. He is involved in national and international research programmes, and in projects in cooperation with industries.

Daniele Marioli was born in Brescia, Italy, in 1946. He obtained the Electrical Engineering degree in 1969. From 1984 to 1989 he was an Associate Professor in Applied Electronics and since 1989 he has been a Full Professor of Electronics at the University of Brescia. His main field of activity is the design and experimentation of analog electronic circuits for the processing of electrical signals from transducers, with particular regard to S/N ratio optimization.

Emilio Sardini was born in Commessaggio, Mantova, Italy in 1958. He graduated in Electronic Engineering at the Politecnico of Milan, Italy, in 1983. Since 1984 he joined the Department of Electronic of Industrial Automation of the University of Brescia, Italy. From 1986 to 1998 he has been an Assistant Professor. Since 1998 he is an Associate Professor in Electrical and Electronics Measurements and recently won a full professor position. He teaches courses in the field of Electronics Instrumentation. His research activity has been addressed to sensors and electronic instrumentation, in particular to the conditioning electronics mainly of capacitive and inductive sensors, microprocessor-based instrumentation, development of thick film sensors, instrumentation for noise and for low frequency acceleration measurements.

Mauro Serpelloni was born in Brescia, Italy, in 1979. He received the Laurea degree summa cum laude in industrial management engineering from the University of Brescia in October 2003. In March 2007 he received the Research Doctorate degree in Electronic Instrumentation at the University of Brescia. He is currently research assistant of Electrical and Electronic Measurements at the Faculty of Engineering of the University of Brescia. He has worked on several projects relating to design, modeling and fabrication of measurement systems for industrial applications. His research interests include especially contactless transmissions between sensors and electronics, contactless activation for resonant sensors and signal processing for microelectromechanical systems.

Andrea Taroni was born in 1942. He received the degree in Physical Science from the University of Bologna, Italy, in 1966. He was an Associate Professor at the University of Modena from 1971 to 1986. Since 1986 he has been Full Professor of Electrical Measurements at the University of Brescia. He has done extensive research in the field of sensors for physical quantities and electronic instrumentation, both developing original devices and practical applications. He is author of more than 100 scientific papers.